Katabatic flow over a differentially cooled slope

By Alan Shapiro, Bryan Burkholder, and Evgeni Fedorovich
School of Meteorology, University of Oklahoma, Norman, Oklahoma

National Weather Center Seminar Series on Boundary Layer, Urban Meteorology, and Land-Surface Processes, 6 December 2010

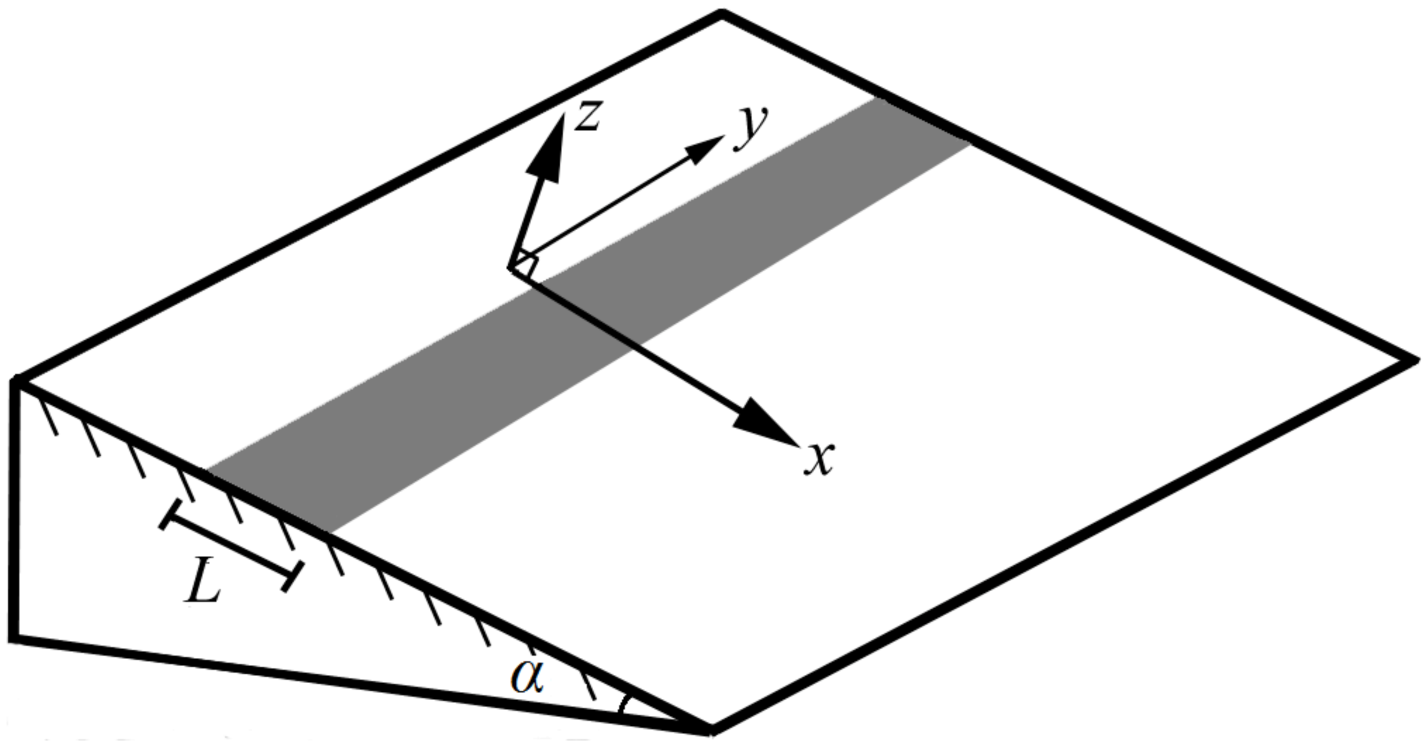

Katabatic flow theory and modeling

1. **Prandtl Slope Model and its Extensions (Prandtl 1942)**

   Exact solution of Navier-Stokes equations for 1D flow down an infinite planar cooled surface in a stably stratified fluid. Good description of mean flow when eddy viscosity is tuned.

2. **Hydraulic Flow Theory (Ball 1956, Doran & Horst 1983)**

   Layer-mean equations are solved with imposed shape factors and entrainment rates. Can be applied to katabatic jumps.

3. **3-D Mesoscale Modeling (many refs, e.g., Renfrew 2004)**

   Strong and weak katabatic flow simulation over complex drainage basins, Greenland and Antarctica ice-sheets.

4. **Large-Eddy Simulation (Skyllingstad 2003)**

   Examined role of turbulence in determining mean flow characteristics in katabatic flow down a cooled cone.

Prandtl's katabatic flow model (1942)

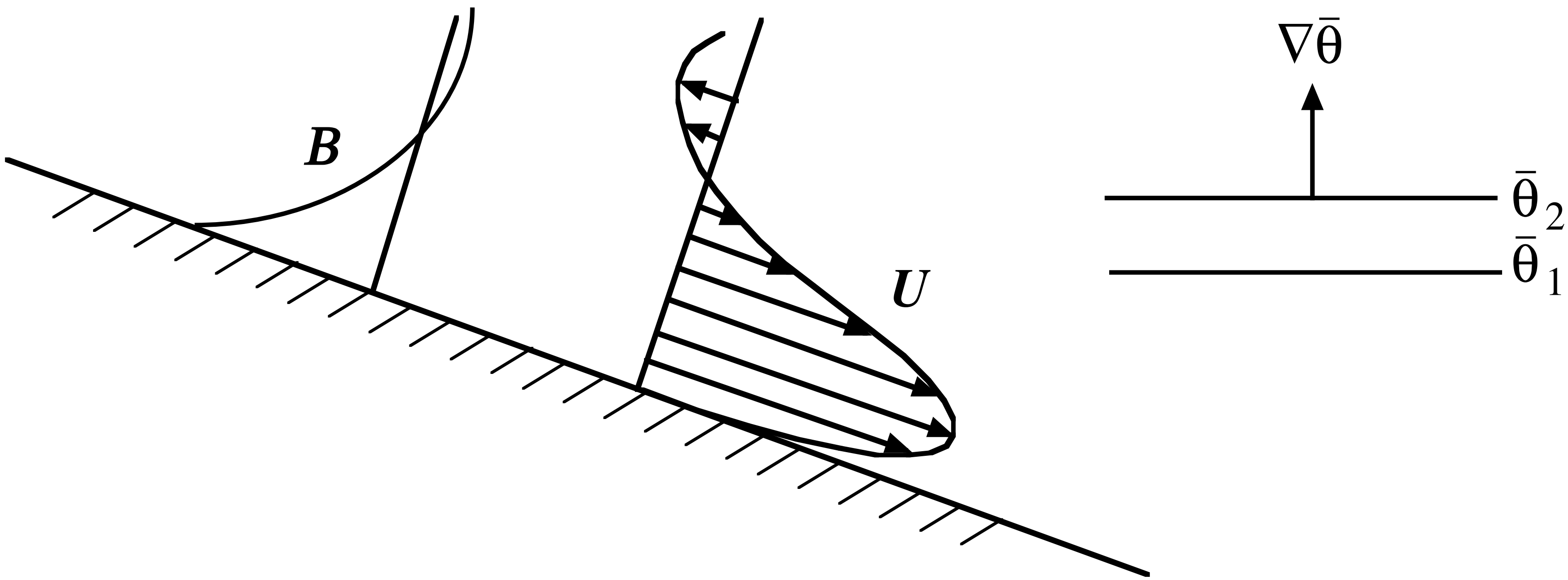

Steady 1-D flow of viscous fluid along a uniformly cooled sloping planar surface in a stably stratified atmosphere.

$$0 = U N^2 \sin\alpha + \kappa \frac{\partial^2 B}{\partial Z^2}, \qquad 0 = -B \sin\alpha + \nu \frac{\partial^2 U}{\partial Z^2}$$

With variables and parameters suitably redefined, this Prandtl katabatic model is identical to the Ekman model (Ekman spiral).

Extensions of the Prandtl model

Gutman & Malbackov (1964), Lykosov & Gutman (1972), Gutman & Melgarejo (1981), Gutman (1983) considered

- Coriolis force
- external pressure gradient force
- time dependence
- simple but non-constant (eddy) viscosities

Grisogono & Oerlemans (2001, 2002) considered general vertical variations in eddy viscosity via the WKB approximation.

Egger (1981), Kondo (1984), Shapiro & Fedorovich (2008) and Axelsen et al. (2010) considered surface thermal inhomogeneity with linearized governing equations.

Shapiro & Fedorovich (2007) and Burkholder et al. (2009) considered surface thermal inhomogeneity within the context of nonlinear models.

Examples of surface thermal inhomogeneities

- Differential cloud cover

- Differential topographic shading (e.g., upper slopes are shaded while lower slopes are sunlit)

- Differential soil moisture (e.g., from variable surface rainfall)

- Isolated patches of snow/ice on a slope

- Variations in snow/ice coverage (e.g., ablation zone of glaciers)

- Variations in vegetation type or coverage

- Variations in land use

Purpose of this study

Develop a simple boundary-layer theory to gain insight into the structure of katabatic flows induced by down-slope-varying thermal forcings.

We focus on top-hat profiles of buoyancy on a planar slope – the simplest geometry to study surface thermal inhomogeneity. This work extends the analyses of Egger (1981), Kondo (1984) and Burkholder et al. (2009).

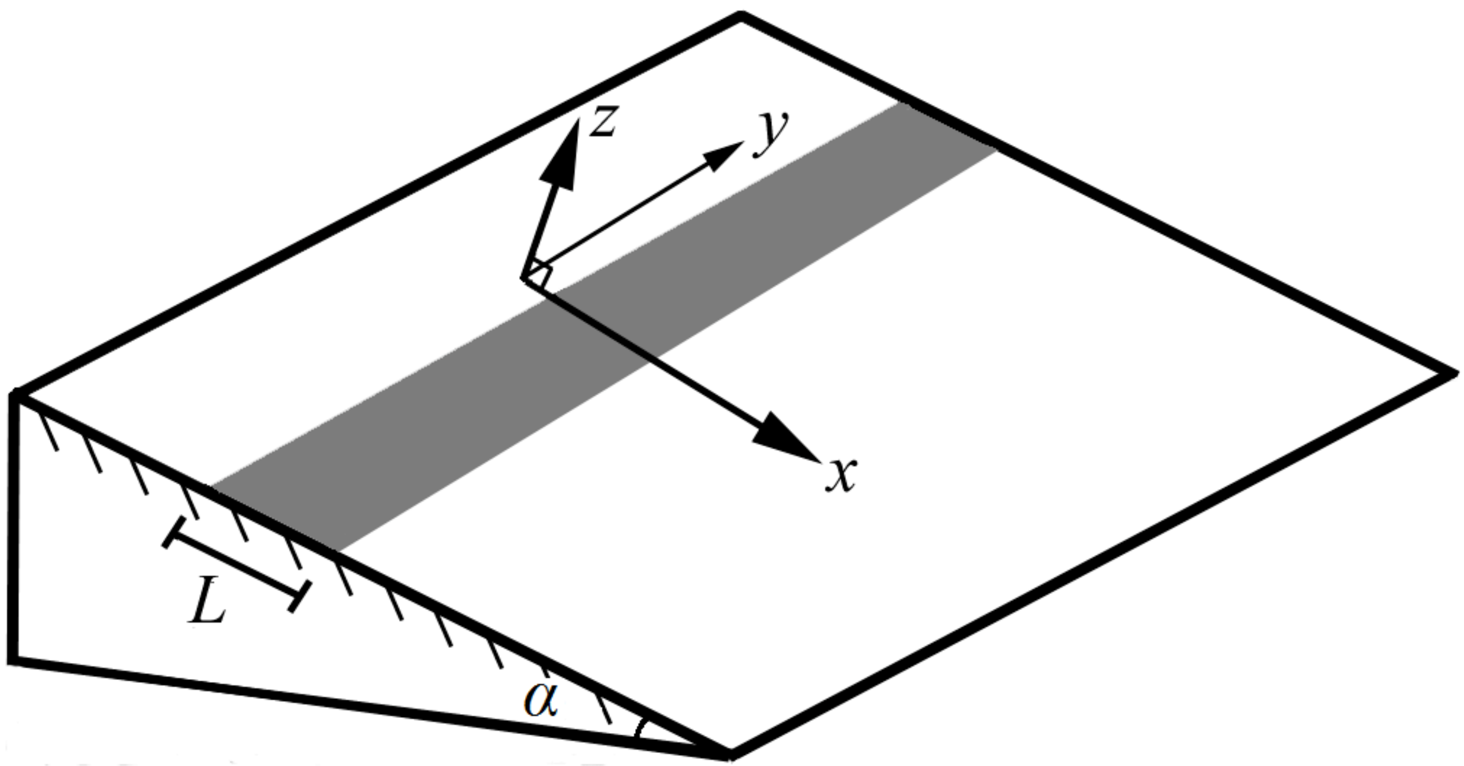

Model assumptions/restrictions

- "Local" katabatic flow – no ambient wind or synoptic-scale p.g.f.
- Steady state
- No Coriolis force
- Linearized Boussinesq dynamics
- Boundary-layer approximation ($\partial^2 U/\partial X^2 << \partial^2 U/\partial Z^2$)
- Hydrostatic
- No cross-slope (Y) variation in buoyancy. This is a 2D problem.
- Constant ν, κ and Brunt-Väisälä frequency $N \equiv \sqrt{(g/\Theta_r) d\Theta_\infty / dZ^*}$.

Slope-following coordinate system

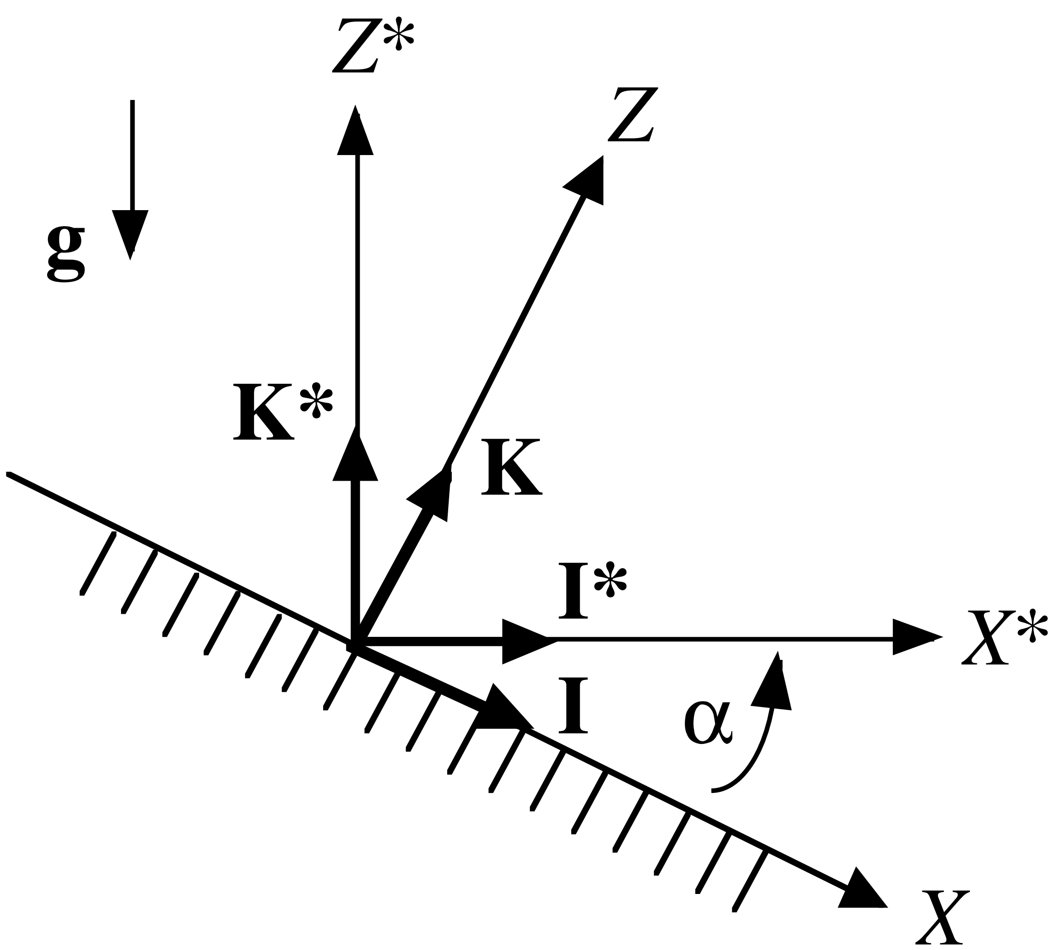

X, Z: along-slope and slope-normal coordinates, respectively.

U, W: along-slope and slope-normal velocity components, respectively.

Linearized boundary-layer equations

Down-slope equation of motion: $$0 = -\frac{\partial \Pi}{\partial X} - B\sin\alpha + \nu \frac{\partial^2 U}{\partial Z^2} \quad (1)$$

Slope-normal equation of motion: $$0 = -\frac{\partial \Pi}{\partial Z} + B\cos\alpha \quad (2)$$

Thermodynamic energy equation: $$0 = UN^2\sin\alpha - WN^2\cos\alpha + \kappa \frac{\partial^2 B}{\partial Z^2} \quad (3)$$

Incompressibility condition: $$\frac{\partial U}{\partial X} + \frac{\partial W}{\partial Z} = 0 \quad (4)$$

$\Pi \equiv (P - P_\infty)/\rho_r$ is normalized pressure perturbation
$B \equiv g(\Theta - \Theta_\infty)/\Theta_r$ is buoyancy; Θ_∞ is environmental potential temperature

Red terms in (1)–(4) were not present in the original 1D Prandtl model. They arise from 2D aspects of the inhomogeneous problem: convergence, slope-normal ascent/descent and slope-normal advection of Θ_∞.

Boundary Conditions

Slope boundary conditions

Impermeability condition: $W(X,0)=0$,

No-slip condition: $U(X,0)=0$,

Specified buoyancy: $B(X,0)=f(X)$,

or

Specified buoyancy flux: $\frac{\partial B}{\partial Z}(X,0)=g(X)$.

Far-above-slope boundary conditions

All variables are bounded as $Z\to\infty$.

Non-dimensional variables

Remove as many parameters as possible from our problem by introducing:

$$x \equiv \frac{X}{X_s}, \quad z \equiv \frac{Z}{Z_s}, \quad u \equiv \frac{U}{U_s}, \quad w \equiv \frac{W}{W_s}, \quad \pi \equiv \frac{\Pi}{\Pi_s}, \quad b \equiv \frac{B}{B_s},$$

where

$$Z_s \equiv \frac{(\nu\kappa)^{1/4}}{(N\sin\alpha)^{1/2}}, \qquad X_s \equiv \frac{(\nu\kappa)^{1/4}\cos\alpha}{N^{1/2}\sin^{3/2}\alpha}, \qquad U_s \equiv \frac{B_s}{N}\left(\frac{\kappa}{\nu}\right)^{1/2},$$

$$W_s \equiv \frac{B_s}{N}\left(\frac{\kappa}{\nu}\right)^{1/2}\frac{\sin\alpha}{\cos\alpha}, \qquad \Pi_s \equiv \frac{B_s(\nu\kappa)^{1/4}\cos\alpha}{(N\sin\alpha)^{1/2}},$$

$$B_s \equiv \begin{cases} \max\limits_{X\in(-\infty,\infty)} \left|B(X,0)\right|, & \text{(if buoyancy is specified),} \\ \max\limits_{X\in(-\infty,\infty)} \left|Z_s\dfrac{\partial B}{\partial Z}(X,0)\right|, & \text{(if buoyancy flux is specified).} \end{cases}$$

Non-dimensional problem

$$0 = -\frac{\partial \pi}{\partial x} - b + \frac{\partial^2 u}{\partial z^2}, \tag{5}$$

$$0 = -\frac{\partial \pi}{\partial z} + b, \tag{6}$$

$$0 = u - w + \frac{\partial^2 b}{\partial z^2}, \tag{7}$$

$$\frac{\partial u}{\partial x} + \frac{\partial w}{\partial z} = 0. \tag{8}$$

Boundary condition for top-hat buoyancy: $$b(x,0) = \begin{cases} -1, & |x| \le l, \\ 0, & |x| > l. \end{cases} \tag{9}$$

Thus, a flow driven by a top-hat forcing (cold strip) is fully characterized by a single parameter, the non-dimensional strip width:

$$l \equiv \frac{L}{X_s} = L \frac{N^{1/2} \sin^{3/2}\alpha}{(\nu\kappa)^{1/4} \cos\alpha}. \tag{10}$$

Reducing the problem to a single ODE

Taking $\partial/\partial z(5) - \partial/\partial x(6)$ eliminates π and yields the vorticity equation:

$$0 = -\ \partial b/\partial x\ -\ \partial b/\partial z\ +\ \partial^2\eta/\partial z^2. \tag{11}$$

Baroclinic generation (proportional to $-\partial b/\partial X^*$)

Diffusion of cross-slope vorticity $\eta = \partial u/\partial z$

Introduce streamfunction ψ defined by $u = \partial\psi/\partial z$, $w = -\partial\psi/\partial x$. The thermodynamic energy and vorticity equations then combine to form:

$$\frac{\partial^2\psi}{\partial x^2} + 2\frac{\partial^2\psi}{\partial x\partial z} + \frac{\partial^2\psi}{\partial z^2} + \frac{\partial^6\psi}{\partial z^6} = 0. \tag{12}$$

Taking the Fourier Transform (FT) of (12) yields the ODE

$$\frac{d^6\hat{\psi}}{dz^6} + \frac{d^2\hat{\psi}}{dz^2} + 2ik\frac{d\hat{\psi}}{dz} - k^2\hat{\psi} = 0, \tag{13}$$

where $\hat{\psi}$ is the FT of ψ.

Solving the ODE

Apply $\hat{\psi} \sim \exp(mz)$ in (13), get the 6th-degree polynomial equation:

$$m^6 = -(i\,k + m)^2 . \tag{14}$$

Taking the square root of (14) yields the cubic equation (well 2 equations),

$$m^3 = \pm\,(i\,m - k)\,. \tag{15}$$

Solve (15) implicitly, by treating it as a linear equation for k. Reject the solutions with Re(m) > 0 to avoid unphysical blow-up of $\hat{\psi}$ (and ψ) far above the slope. The general solution for $\hat{\psi}$ can then be written as

$$\hat{\psi} = n_1 \exp(m_1 z) + n_2 \exp(m_2 z) + n_3 \exp(m_3 z), \tag{16}$$

where n_1, n_2, n_3 are fixed by the slope boundary conditions. Get ψ by evaluating the inverse FT of (16).

Top-hat results for large l

Contour plots of ψ and b show that for large and increasing l, all flow structures became independent of l – so one solution fits all large-l cases.

ψ for $l = 75$

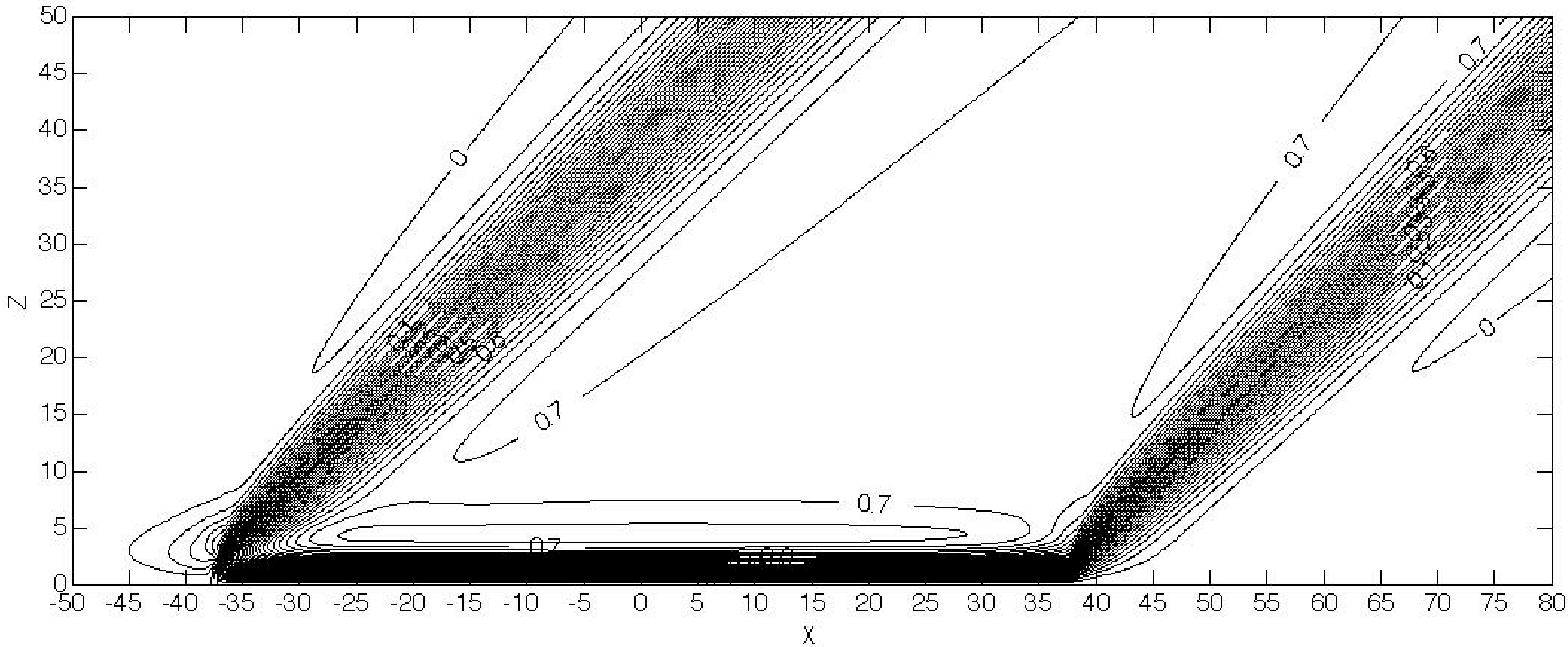

Top-hat results for $l = 25$

$\psi \rightarrow$

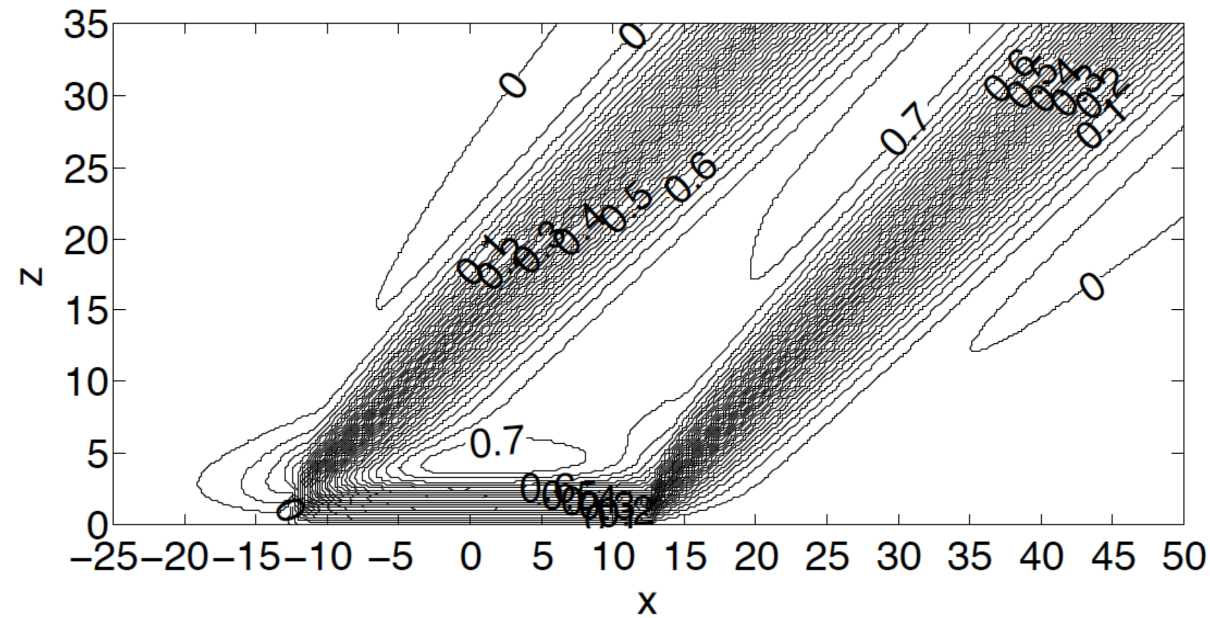

$b \rightarrow$

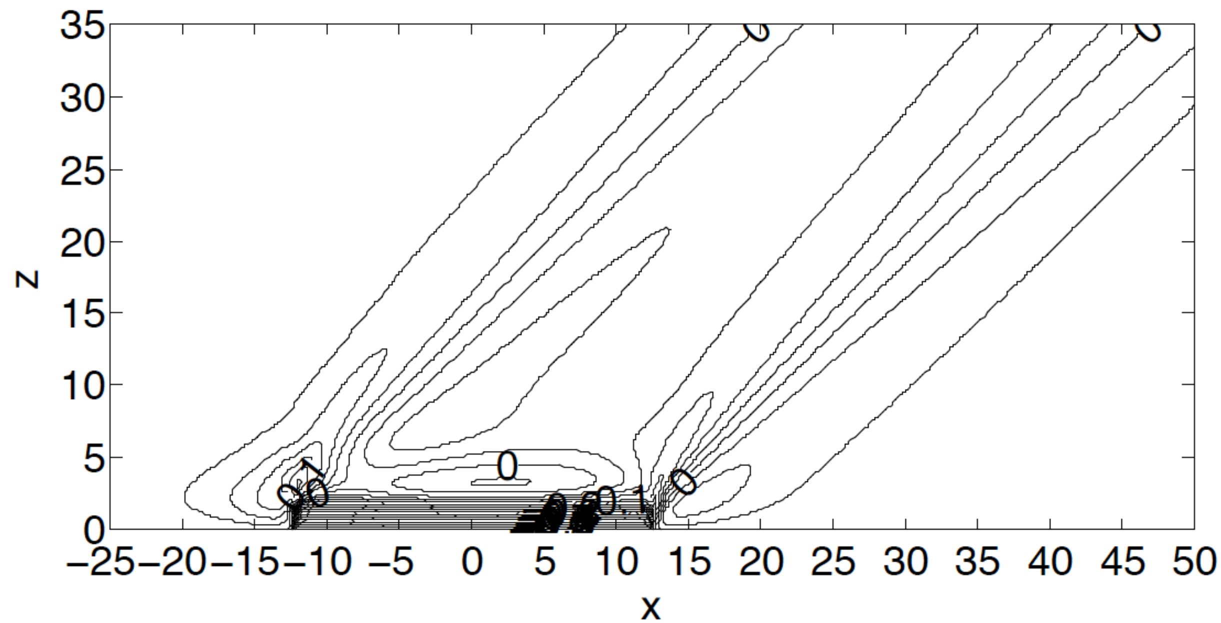

Close-up view of upslope edge of cold strip (*l* = 25)

$\psi \rightarrow$

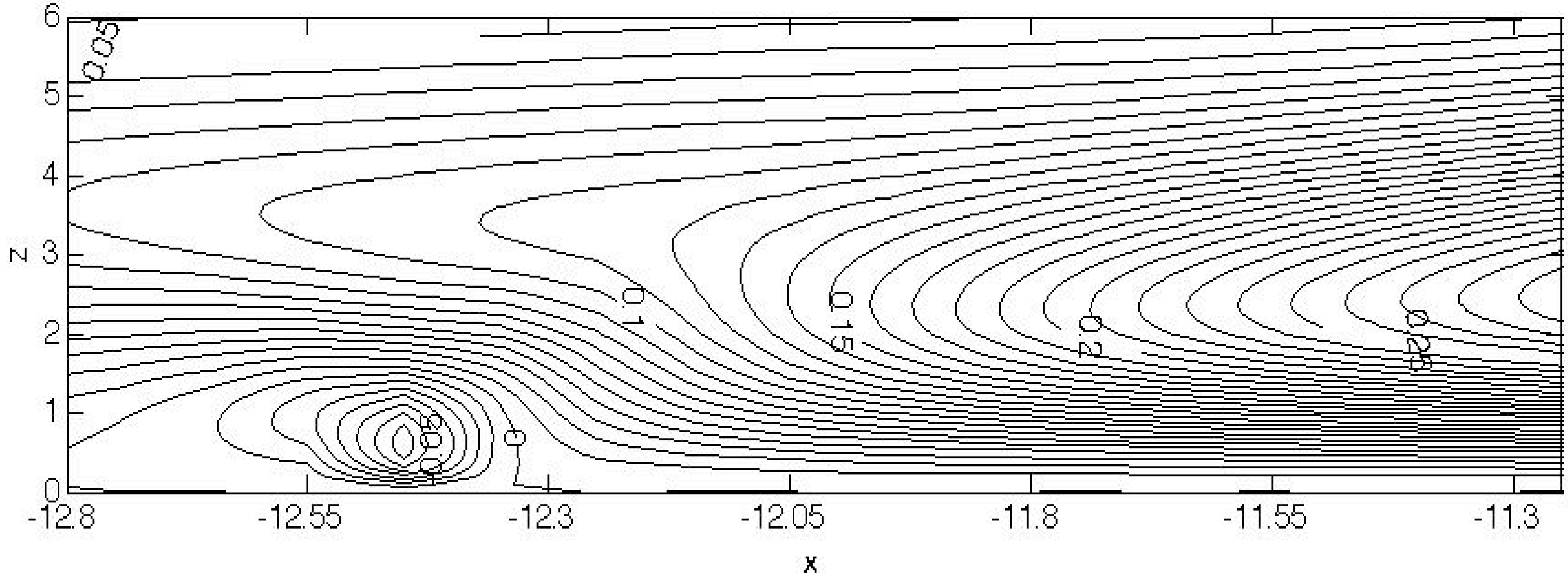

$b \rightarrow$

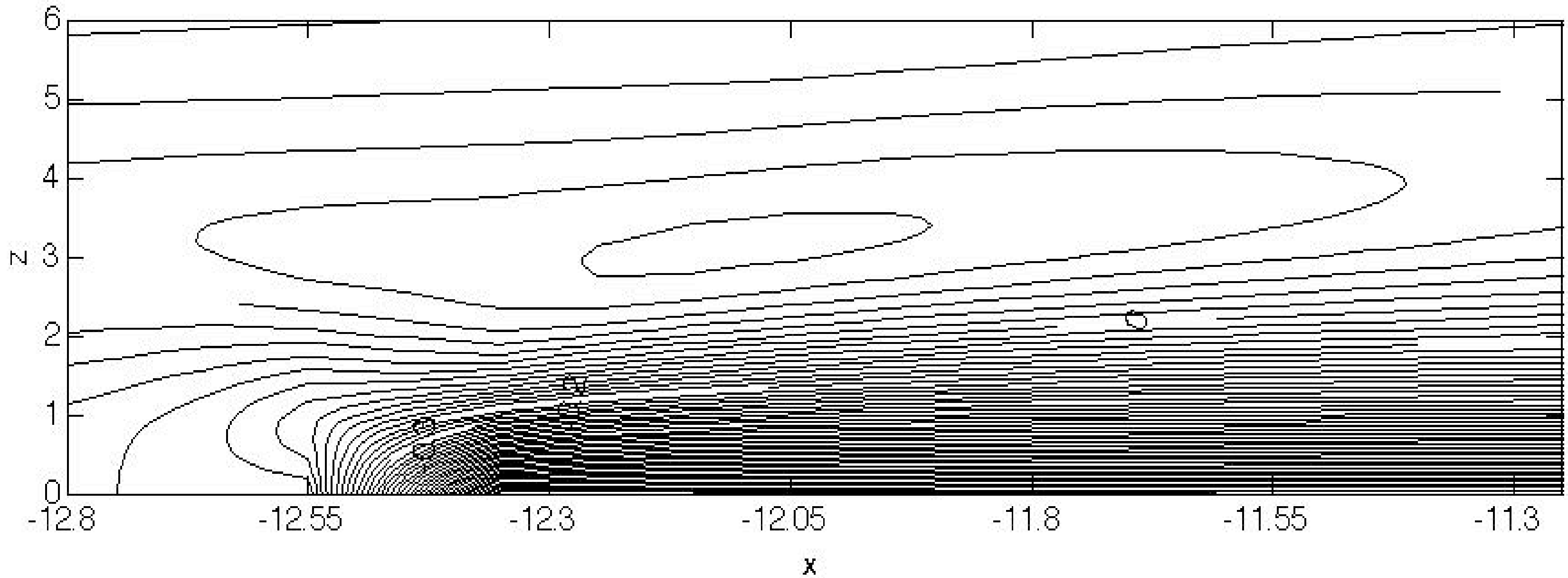

Vorticity dynamics of the horizontal inflow jet

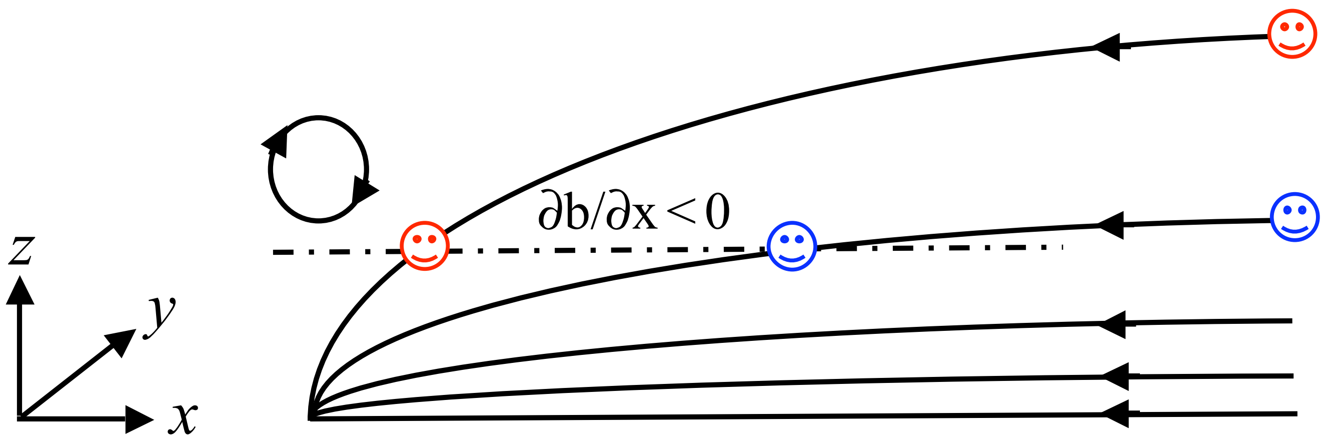

Positive y-component vorticity ($\eta > 0$) is generated baroclinically.

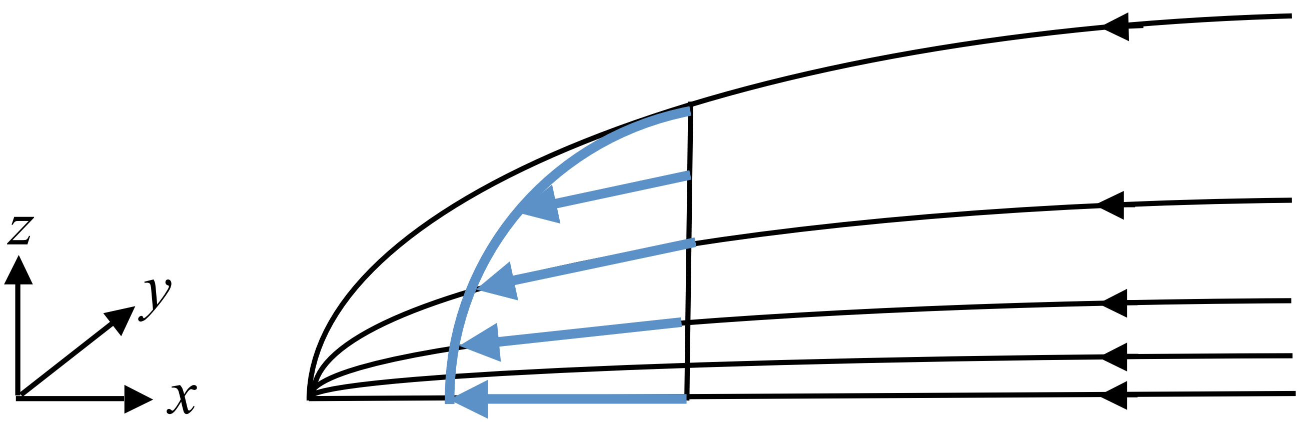

Get balance between diffusion of η and baroclinic generation of η.

Inflow jet as a viscous selective withdrawal layer

The inflow jet is visually similar to flow of a viscous stably stratified fluid towards a line sink (Koh 1966). Preliminary analysis suggests the jet is well described by the same similarity model as in the sink problem, that is:

$$u \sim \frac{1}{x^{1/3}} g(\zeta), \qquad w \sim \frac{1}{x^{1/3}} h(\zeta), \qquad \text{where} \qquad \zeta \equiv \frac{z}{x^{1/3}}.$$

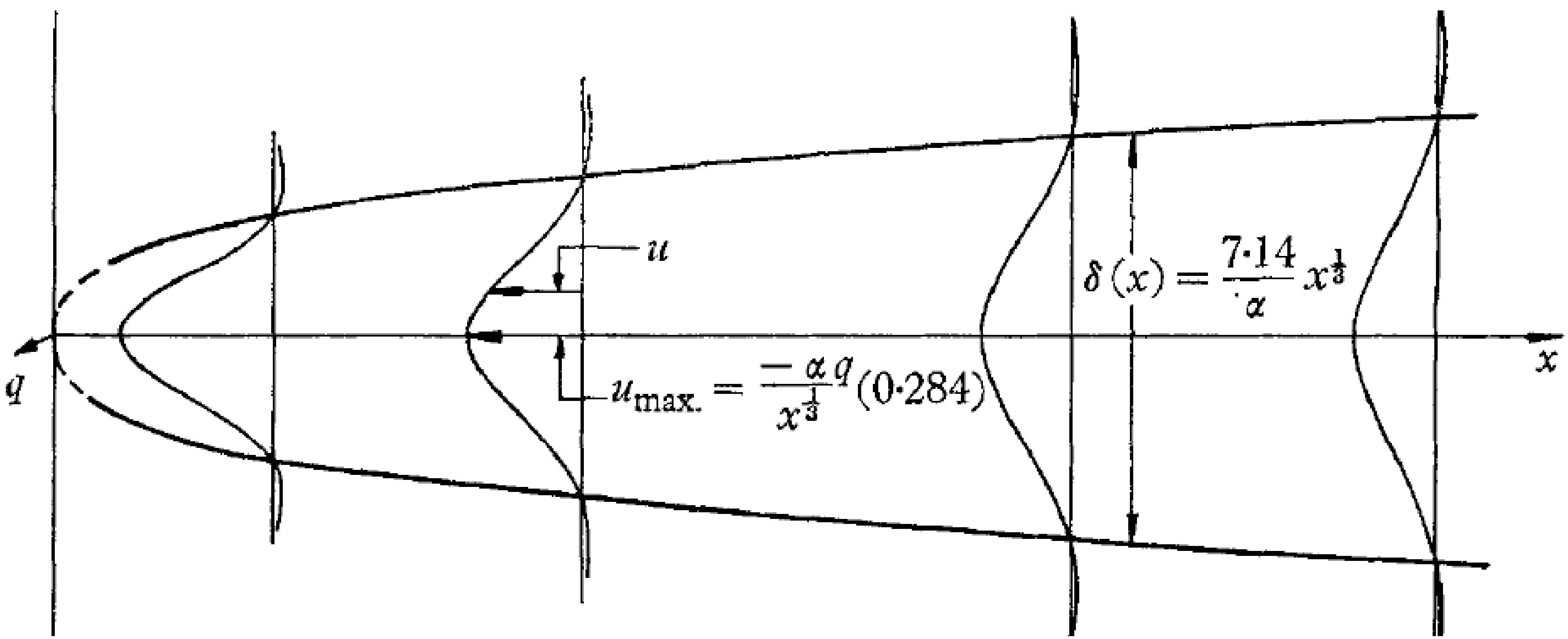

Direct numerical simulation (DNS)

The nonlinear initial value problem for a suddenly imposed top-hat cold strip was solved via DNS. Experiments were performed to

- verify analytical work (weak thermal disturbance)
- explore non-linear aspects of the flow (strong thermal disturbance)
- examine transient solution leading to the steady state

The simulations required <u>lots</u> of grid points because:

- a very high resolution was needed to resolve the shallow katabatic jet
- a very tall and wide domain was needed to delay the interaction of inflow/outflow jets and gravity waves with computational boundaries

DNS code was a parallel version of code used by Fedorovich et al. (2001), Shapiro & Fedorovich (2004, 2006, 2007), and Burkholder et al. (2009).

Parameters for $l \sim 40$ experiment

Physical Parameters:

Slope angle:	$\alpha = 15°$
Slope temperature perturbation:	$\Delta T = 3$ K
Length of cold strip:	$L \sim 2.8$ km
Brunt-Väisälä frequency:	$N = 0.01$ s^{-1}
Eddy viscosity/diffusivity:	$\nu = \kappa = 1$ m^{2}s^{-1}

Computational Parameters:

Domain height:	$h = 8$ km
Domain width:	$d \sim 32.7$ km
Grid spacing:	$\Delta X = \Delta Z = 2$ m

Ψ and b at $t \sim 81$ min

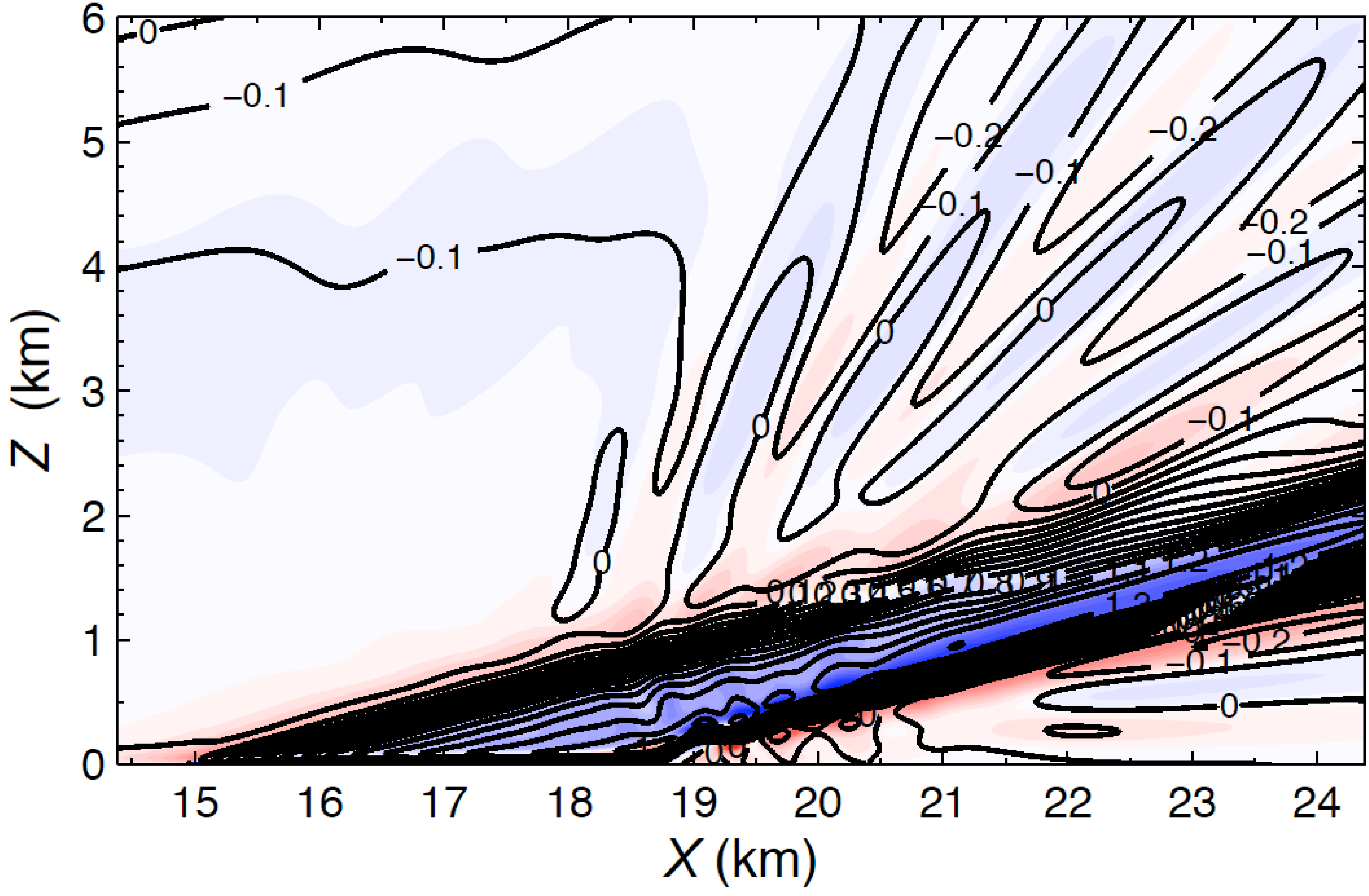

Zoomed-in view at $t = 81$ min

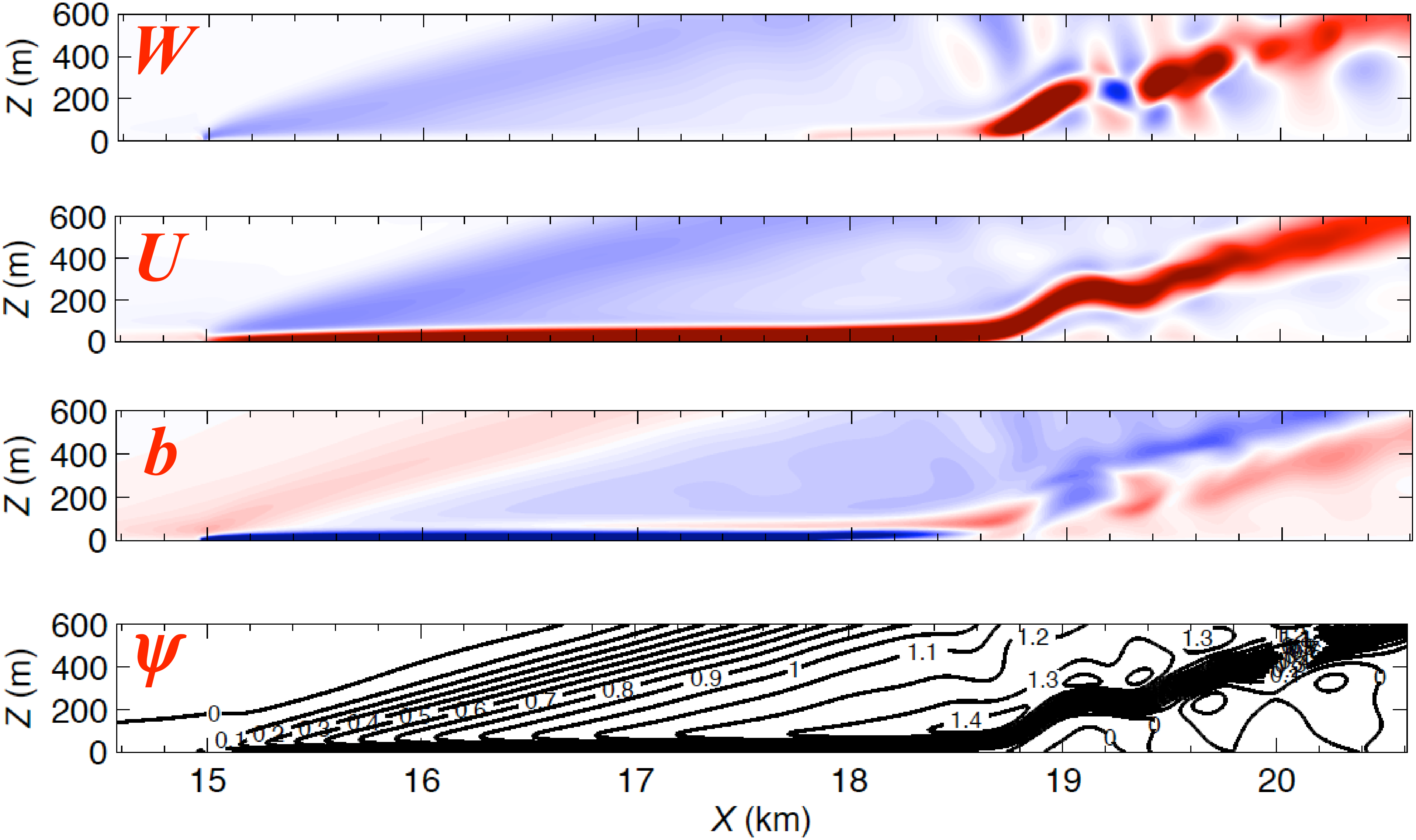

$U(Z)$ profiles at select locations along the cold strip

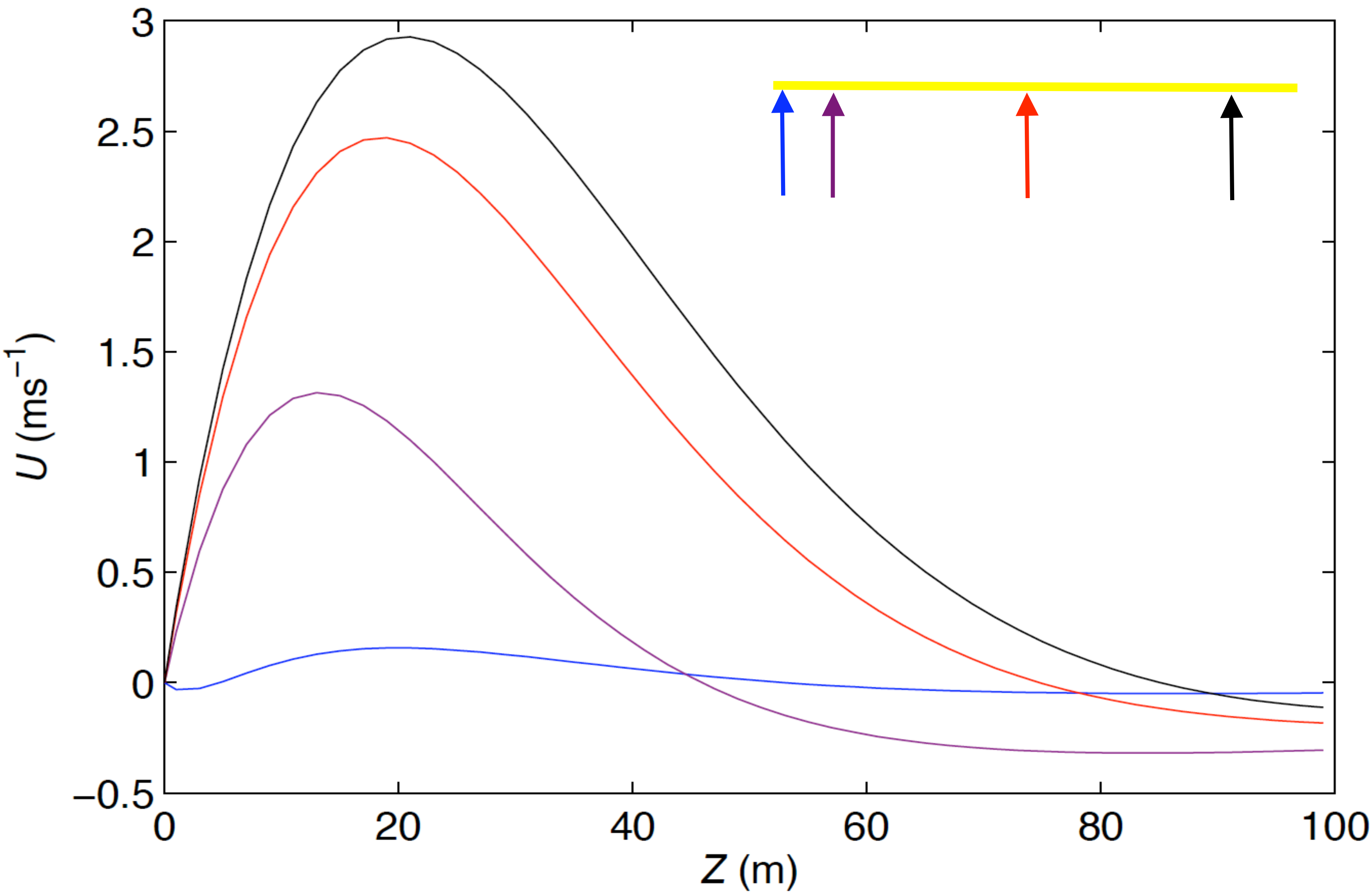

Compate with Prandtl solution: Jet height $\approx 21.8\text{m}$, peak $U \approx 3.22\ \text{ms}^{-1}$

Summary

The linear problem is governed by a single parameter, the strip width l. For large l, flow structures become independent of l, and scale as:

$$Z_i \sim \frac{(\nu\kappa)^{1/4}}{(N\sin\alpha)^{1/2}}, \quad X_i \sim \frac{(\nu\kappa)^{1/4}\cos\alpha}{N^{1/2}\sin^{3/2}\alpha}, \quad U_i \sim \frac{B_s}{N}\left(\frac{\kappa}{\nu}\right)^{1/2}, \quad W_i \sim \frac{B_s}{N}\left(\frac{\kappa}{\nu}\right)^{1/2}\frac{\sin\alpha}{\cos\alpha}$$

Key features in linear solution:

- primary katabatic jet
- inflow and outflow jets flowing horizontally toward/away from slope
- low level rotor in baroclinic zone on upslope edge of cold strip
- warm thermal belt above upslope edge of cold strip

DNS results are similar to linear results but with some notable differences:

- Prandtl regime delayed down the strip
- advection brings cold air down-slope off strip
- outflow jet is narrower and more intense than inflow jet
- a stationary gravity wave where primary jet erupts into outflow jet